# ChemComm

Accepted Manuscript


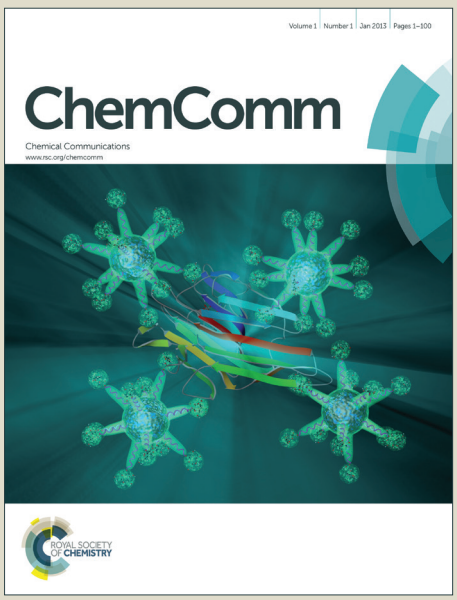





ROYAL SOCIETY OF CHEMISTRY

www.rsc.org/chemcomm

Journal Name

RSCPublishing

COMMUNICATION

# An Aggregation-Induced Emission (AIE) Active Probe Renders Al(III) Sensing and Tracking of Subsequent Interaction with DNA

Soham Samanta,[a] Sudeep Goswami,[b] Md. Najbul Hoque,[a] Aiyagari Ramesh*,[b] and Gopal Das*,[a]

Cite this: DOI: 10.1039/x0xx00000x

Received ooth January 2012,
Accepted ooth January 2012

DOI: 10.1039/x0xx00000x

www.rsc.org/

**An aggregation-induced emission (AIE) active probe (L) displayed TURN-ON fluorescence response toward $Al^{3+}$ in physiological condition and in HeLa cells. The L-$Al^{3+}$ ensemble could subsequently facilitate tracking of interaction with DNA in solution.**

Aluminium is the third most abundant metal in the earth's crust and is widely acknowledged as a neurotoxic agent. Aluminium-associated toxicity has been implicated in impairment of the central nervous system and neurodegenerative diseases such as Alzheimer's.[1-4] Owing to its significant impact on the biosphere and human health, development of sensors for rapid and sensitive detection of $Al^{3+}$ has stimulated great scientific interest amongst chemists at large. Fluorescence-based systems are considered to be pertinent in the context of sensing of biological and environmentally relevant metal ions as they can afford rapid, convenient and sensitive detection of target analytes. [5-10] In the domain of aluminium sensing, fluorescence TURN-ON chemosensors have been described, wherein the mechanism of sensing has been largely attributed to internal charge transfer (ICT), chelation-enhanced fluorescence (CHEF), photo-induced electron transfer (PET) or fluorescent resonance energy transfer (FRET). [11-18] In recent years, fluorescent probes that display aggregation-induced emission (AIE) have come to limelight. These probes display a weak emission in dilute solution, which is subsequently enhanced manifold as a consequence of aggregation of the fluorophore species driven by probe-target interaction in solution or solid state and thus AIE active probes are perceived to be attractive candidates for robust and quantitative sensing of various target analytes. [19-23] It is also conceivable that the emission of an AIE-based system is likely to be responsive to an additional competing species that can modulate the probe-target interaction, thereby enabling the probe to render dual sensing. Based on this rationale, here in we describe an AIE- active Schiff base probe L (Scheme 1), which displays a selective fluorescence TURN-ON response toward $Al^{3+}$ and interestingly the subsequent interaction of L-Al ensemble with DNA could be captured through a systematic fluorescence TURN-OFF response of the highly emissive ensemble.

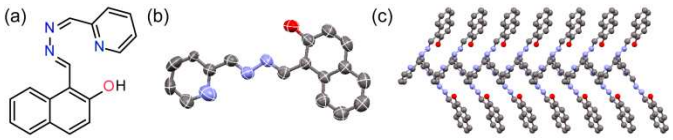


Scheme 1. (a) Molecular structure, (b) ORTEP plot and (c) packing diagram of L.

UV–Vis spectra of L revealed two absorption maxima at 334 nm (π–π*) and 384 nm (n–π*) in $CH_3OH$/aqueous HEPES buffer (5 mM, pH 7.3; 9:1, v/v). The selectivity of L was checked with chloride or nitrate salts of various metal ions which included $Na^+$, $K^+$, $Ca^{2+}$, $Mg^{2+}$, $Cr^{3+}$, $Hg^{2+}$, $Cu^{2+}$, $Pb^{2+}$, $Zn^{2+}$, $Fe^{3+}$, $Al^{3+}$, $Co^{2+}$, $Ni^{2+}$, $Cd^{2+}$ and $Ag^+$. The presence of $Cu^{2+}$ could be detected by UV-visible absorbance spectroscopy (Figure 1A and ESI†, Figure S5) with a detection limit of 1.095 nM, (ESI†, Figure S7). Amongst the metals tested, $Al^{3+}$ and $Co^{2+}$ were also able to induce colorimetric changes (Figure 1A). Fluorescence spectra of L revealed a weak emission band at 506 nm on excitation at 400 nm in $CH_3OH$/aqueous HEPES buffer (5 mM, pH 7.3; 9:1, v/v). Interestingly amongst all tested metal ions only $Al^{3+}$ rendered a remarkable TURN-ON fluorescence response with a 31 nm red shifted new peak emerging at 537 nm along with a manifold increase in fluorescence intensity (Figure 1B, ESI†, Figure S9). Furthermore, naked eye detection of this selective TURN-ON response of L toward $Al^{3+}$ was also feasible under UV light, which rendered a bright yellowish green fluorescence (Figure 1B INSET). Interestingly no other metal ions interfered with the TURN-ON fluorescence response of L in presence of $Al^{3+}$ (ESI†, Figure S10), which expands the scope of the sensor for specific detection of $Al^{3+}$. Incremental addition of $Al^{3+}$ ions resulted in a systematic increase in the emission intensity of L with a gradual red shift in emission maxima (Figure 1C). Mass spectrum analysis (ESI†, Figure S11) confirmed the formation of 1:1 L-$Al^{3+}$ complex with the generation of molecular ion peak at m/z=391.2 ($[Al+L+H_2O+2Cl]^+$). Detection limit

Journal Name RSCPublishing

## COMMUNICATION

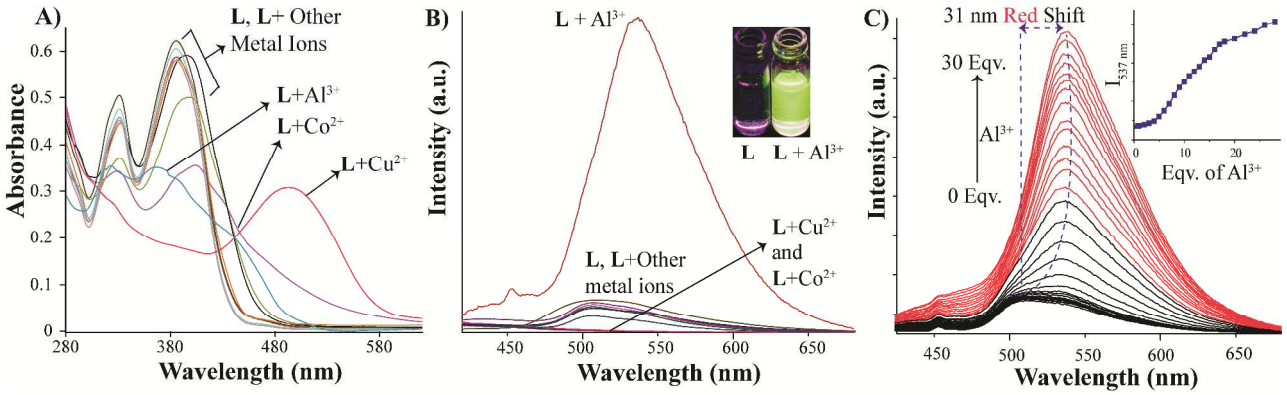


Figure 1. (A) UV-Visible spectra of **L** (10 μM) in presence of different metal ions in mixed solvent. (B) Fluorescence spectra of **L** in presence of 10 equivalents of various metal ions. INSET: Visual changes observed for **L** in absence and in presence of $Al^{3+}$ under UV light. (C) Fluorescence spectra of **L** (10 μM) with varying concentration of $Al^{3+}$. $\lambda_{ex}$ = 400 nm. INSET: Emission intensity change at 537 nm with concentration of $Al^{3+}$.

for $Al^{3+}$ was found to be ~2.8 μM (ESI†, Figure S12), which is well below the permissible level of $Al^{3+}$ in drinking water according to the USEPA.

Interestingly it was observed that the weakly emissive L in pure methanol became highly emissive when a suspension was formed in methanol-water mixture (ESI†, Figure S13). This observation suggested that L is an AIE-active compound. It may be mentioned here that the crystal structure of the compound also supports the propensity of the ligand to form aggregation via non-covalent interaction (Scheme 1, ESI†, Figure S14). Presumably, metal chelation is involved in the selective turn on fluorescence. However, fluorescence titration experiment failed to indicate the 1:1 complex formation as the fluorescence intensity increased linearly up to addition of 30 equivalents of $Al^{3+}$ (Figure 1C). Thus it may be assumed that along with formation of complex, $Al^{3+}$ also helped to form aggregates in the solution when added in excess, which in turn triggered the AIE activity of L (Scheme 2).

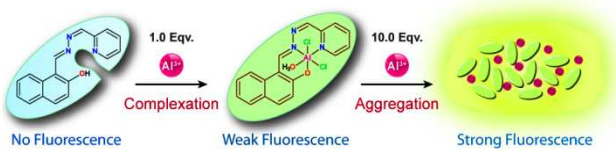


Scheme 2. Plausible mechanism of complexation and $Al^{3+}$ induced aggregation of L.

Initial complexation resulted in the enhanced fluorescence intensity along with red shift in maxima as the chelation inhibited the free rotation and increased the delocalization of the ligand. However, further addition of $Al^{3+}$ from 2.0 to 30 equivalents initiated the aggregation of already formed complex, a phenomenon which manifested as a dramatic enhancement in fluorescence intensity due to AIE activation.

Dynamic light scattering (DLS) studies of L in a mixed aqueous media suggested that the average particle size increased from 333 nm to 1140 nm on changing the $Al^{3+}$ concentration from 1.0 equivalent to 10 equivalents, which also supports the observed $Al^{3+}$-triggered AIE activity of the compound (Figure 2A). Atomic force microscope (AFM) and field emission scanning electron microscope (FESEM) analysis provided additional evidences for the formation of aggregates of L-Al complex (Figure 2B-2C). It is significant to mention here that AIE was observable only when the water fraction in the medium reached the threshold of 80% and above (Figure 2D, ESI†, Figure S13). Addition of appropriate amount of EDTA solution restored the native fluorescence of L when added to the highly fluorescent $Al^{3+}$-treated L, which substantiated the role of $Al^{3+}$ in triggering aggregation and that aggregation was initiated after complex formation (ESI†, Figure S15). Detailed theoretical calculations also supported this premise. Density functional calculation(s) of L, L-$Al^{3+}$ complex and L-$Cu^{2+}$ complex were carried out to ascertain the effect of chelation on spectroscopic signatures. The substantial decrease in the HOMO to LUMO energy gap on chelation of L with $Al^{3+}$ clearly testified the theoretical basis of the observed red shift in emission maxima of L when treated with $Al^{3+}$ (ESI†, Figure S16). A similar decrease in HOMO to LUMO energy gap in the case of $Cu^{2+}$ complex of L compared to L alone (ESI†, Figure S17) also explains the prominent red shift in UV-visible maxima (ESI†, Figure S5). All the optimized structures and their energy levels, which are directly influencing the spectral outcome, are indicated in the supporting information (ESI†, Figure S18, Table S1).

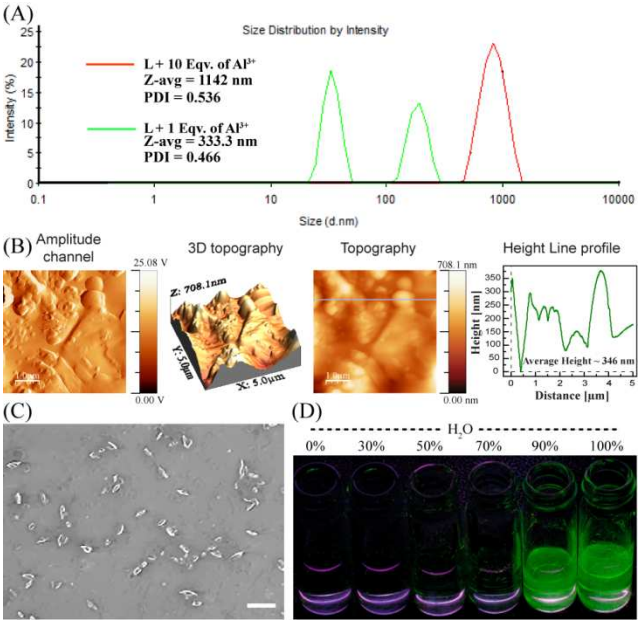


Figure 2. (A) DLS-based particle size analysis upon addition of 1.0 equivalent of $Al^{3+}$ (green) and 10 equivalent of $Al^{3+}$ (red) to **L** in mixed aqueous media. (B) AFM image and (C) FESEM image of the aggregates obtained after addition of $Al^{3+}$ (10 equivalent) to **L**. (D) Visual change observed with increase in percentage of water (0–100%) to a 10 **µ**M solution of L as seen under UV light.

The selective sensing property of L towards $Al^{3+}$ was encouraging and it indicated that the ligand could perhaps be exploited as a fluorescence-based probe for intracellular sensing of $Al^{3+}$. However, to pursue this objective it was paramount to initially verify the cytotoxic effect of L and its $Al^{3+}$ complex on cells. To this end, an MTT assay revealed that the ligand L, $Al^{3+}$ as well as the L-$Al^{3+}$ complex did not influence the viability of cultured HeLa cells even at the highest tested concentration of 96 µM (ESI†, Figure S19). Given the non-toxic nature of L and L-$Al^{3+}$ complex, intracellular detection of $Al^{3+}$ was pursued. Fluorescence microscopic analysis indicated that HeLa cells treated with ligand L alone did not exhibit any intracellular fluorescence emission (Figure 3A). Furthermore, retention of the distinctive morphology of HeLa cells treated with the ligand was observed in the bright field image (Figure 3A), which validated the non-toxic nature of the ligand established earlier in MTT assay (ESI†, Figure S19). Interestingly, when ligand-pretreated HeLa cells were incubated

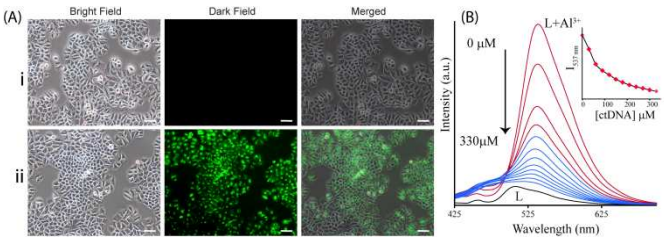


Figure 3. (A) Fluorescence microscope images of HeLa cells (under blue light) for (i) cells treated with 5.0 µM of **L**, (ii) cells pre-treated with 5.0 µM of **L** followed by addition of 50 µM $Al^{3+}$ solutions. Scale bar for the images is 100 µm. (B) Change in emission spectra of L+ $Al^{3+}$ ensemble with varying concentration of ctDNA, $\lambda_{ex}$ = 400 nm. INSET: Changes in the emission intensity at 537 nm with incremental addition of ctDNA.

with hydrated $Al^{+3}$ salt, a significant TURN-ON fluorescence emission was manifested (Figure. 3A). This suggested that the ligand L could translocate across the membrane and render selective sensing of $Al^{3+}$ within HeLa cells. Given the neurotoxic implications of $Al^{3+}$, this finding is significant and it enhances the analytical merit of the ligand as a non-invasive probe for intracellular sensing of $Al^{3+}$. Studies on the interaction between $Al^{3+}$ and DNA hold significant interest as reports suggest that the potential toxicity of $Al^{3+}$ may be associated with its DNA binding property. [24-25] We envisaged that the L-$Al^{3+}$ ensemble is likely to interact with DNA, given the high affinity of $Al^{3+}$ for phosphate groups and this event could be tracked through the change in the emissive response of the AIE active probe. Interestingly, incremental addition of calf-thymus DNA (ctDNA) to the highly fluorescent L-$Al^{3+}$ ensemble solution resulted in a dose-dependent fluorescence quenching (Figure 3B), which suggested disaggregation of L-$Al^{3+}$ ensemble. It is plausible that given the high affinity of $Al^{3+}$ for phosphate groups present in ctDNA, interaction of L-$Al^{3+}$ ensemble with ctDNA and subsequent sequestration of $Al^{3+}$ may ensue, analogous to the interaction of the metal chelator EDTA with L-$Al^{3+}$ ensemble (ESI, Fig. S15). This phenomenon perhaps manifests as disaggregation of the L-$Al^{3+}$ ensemble upon interaction with ctDNA and reduction in AIE activity of L.

In summary we developed a new AIE-active fluorophore that selectively exhibited a TURN-ON fluorescence response towards $Al^{3+}$ in solution and rendered non-invasive detection of $Al^{3+}$ in live HeLa cells. The assimilation of facile $Al^{3+}$ sensing and subsequent tracking of DNA interaction in a single AIE-active system significantly enhances the scope of the developed chemosensor to probe the cellular and molecular basis of $Al^{3+}$ toxicity in future investigations.

We thank CSIR (01/2727/13/EMR-II), Science & Engineering Research Board (SR/S1/OC-62/2011) and Department of Biotechnology (BT/01/NE/PS/08) for research grants, Central Instruments Facility, IIT Guwahati, for AFM and FESEM analysis and Centre for Nanotechnology, IIT Guwahati for DLS analysis. SS and NH thank IIT Guwahati and SG thanks UGC for a research fellowship.

## Notes and references

[a] Department of Chemistry, Indian Institute of Technology Guwahati, Guwahati 781039, India. Fax: + 91 361 2582349; Tel: +91 3612582313; E-mail: gdas@iitg.ernet.in.
[b] Department of Biotechnology, Indian Institute of Technology Guwahati, Guwahati 781039, India. Fax: +91 361 2582249; Tel: +91 361 2582205; E-mail: aramesh@iitg.ernet.in.
Electronic Supplementary Information (ESI) available: [Experimental section and supporting plot and figures]. See DOI: 10.1039/c000000x/

1 A. Salifoglou, *Coord. Chem. Rev.*, 2002, **228**, 297.
2 M. E. Percy, T. P.A. Kruck, A. I. Pogue and W. J. Lukiw, *J. Inorg. Biochem.*, 2011, **105**, 1505.
3 G. D. Fasman, *Coord. Chem. Rev.*, 1996, **149**, 125.
4 D. Krewski, R. A. Yokel, E. Nieboer, D. Borchelt, J. Cohen, J. Harry,

S. Kacew, J, Lindsay, A. M. Mahfouz and V. Rondeau, *J. Toxicol.*
*Environ. Health, Part B: Crit. Rev.*, 2007, **10:S1**, 1.
5 G. Aragay, J. Pons and A. Merkoc, *Chem. Rev*. 2011, **111**, 3433.
6 K. M. Dean, Y. Qin and A. E. Palmer, *Biochim. Biophys. Acta*, 2012, **1823**, 1406.
7 S. Samanta, S. Goswami, A. Ramesh and G. Das, *Sens. Actuators B*., 2014, **194**, 120.
8 B. K. Datta, S. Mukherjee, C. Kar, A. Ramesh and G. Das, *Anal. Chem*., 2013, **85**, 8369.
9 C. Kar, M. D. Adhikari, A. Ramesh and G. Das, *Inorg. Chem.*, 2013, **52**, 743.
10 B. K. Datta, D. Thiyagarajan, C. Kar, A. Ramesh and G. Das, *Org. Biomol. Chem.*, 2014, **12**, 4975.
11 H. M. Park, B. N. Oh, J. H. Kim, W. Qiong, I. H. Hwang, K. Jung, C. Kim and J. Kim, *Tet. Lett*., 2011, **52**, 5581.
12 D. Maity and T. Govindaraju, T., *Chem. Commun*. 2010, 4499.
13 S. H. Kim, H. S. Choi, J. Kim, S. J. Lee, D. T. Quang and J. S. Kim, *Org. Lett*., 2010, **12**, 560.
14 Y. Lu, S. Huang, Y. Liu, S. He, L. Zhao and X. Zeng, *Org. Lett*., 2011, **13**, 5274.
15 M. Arduini, F. Felluga, F. Mancin, P. Rossi, P. Tecilla, U. Tonellato and N. Valentinuzzi, *Chem. Commun*. 2003, 1606.
16 T. H. Ma, M. Dong, Y. M. Dong, Y. W. Wang and Y. Peng, *Chem. Eur. J*., 2010, **16**, 10313.
17 W. H. Ding, W. Cao, X. J. Zheng, D. C. Fang, W. T. Wong and L. P. Jin, *Inorg. Chem.* 2013, **52**, 7320.
18 X. Sun, Y. W. Wang, and Y. Peng, *Org. Lett.*, 2012, **14**, 3420.
19 J. Luo, Z. Xie, J. W. Y. Lam, L. Cheng, H. Chen, C. Qiu, H. S. Kwok, X. Zhan, Y. Liu, D. Zhu and B. Z. Tang, *Chem. Commun.*, 2001, 1740.
20 Y. Hong, J. W. Y. Lam and B. Z. Tang, *Chem. Commun*., 2009, 4332.
21 Y. Hong, J. W. Y. Lam and B. Z. Tang, *Chem. Soc. Rev.*, 2011, **40**, 5361.
22 Y. Liu, Y.Tang, N. N. Barashkov, I. S. Irgibaeva, J. W. Y. Lam, R. Hu, D. Birimzhanova, Y. Yu and B. Z. Tang, *J. Am. Chem. Soc*., 2010, **132**, 13951.
23 X. Chen, X. Y. Shen, E. Guan, Y. Liu, A. Qin, J. Z. Sun and B. Z. Tang, *Chem. Commun.,* 2013, **49**, 1503.
24 J. Wu, F. Du, P. Zhang, I. A. Khan, J. Chen and Y. Liang, *J. Inorg. Biochem*., 2005, **99**, 1145.
25 M. L. Hegde, S. Anitha, K. S. Latha, M. S. Mustak, R. Stein, R. Ravid and K. S. J. Rao, *J. Mol. Neurosci*., 2003, **22**, 19.



 